

## Fast $K^+$ currents from cerebellum granular cells are completely blocked by a peptide purified from *Androctonus australis* Garzoni scorpion venom

Marzia Pisciotto <sup>a</sup>, Fredy I. Coronas <sup>b</sup>, Carlos Bloch <sup>c</sup>, Gianfranco Prestipino <sup>a,1,\*</sup>,  
Lourival D. Possani <sup>b,1,2</sup>

<sup>a</sup> Istituto di Cibernetica e Biofisica, C.N.R., via De Marini 6, 16149 Genova, Italy

<sup>b</sup> Biotechnology Institute-UNAM, Av. Universidad 2001, Cuernavaca 62210, Mexico

<sup>c</sup> EMBRAPA/Cenagen, P.O. Box 02372, Brasilia, DF, Brazil

Received 22 February 2000; received in revised form 25 May 2000; accepted 7 June 2000

### Abstract

A novel peptide was purified from the venom of the scorpion *Androctonus australis* Garzoni (abbreviated Aa1, corresponding to the systematic number alpha KTX4.4). It contains 37 amino acid residues, has a molecular mass of 3850 Da, is closely packed by three disulfide bridges and a blocked N-terminal amino acid. This peptide selectively affects the  $K^+$  currents recorded from cerebellum granular cells. Only the fast activating and inactivating current, with a kinetics similar to  $I_A$ -type current, is completely blocked by the addition of low micromolar concentrations ( $K_i$  value of 150 nM) of peptide Aa1 to the external side of the cell preparation. The blockade is partially reversible in our experimental conditions. Aa1 blocks the channels in both the open and the closed states. The blockage is test potential independent and is not affected by changes in the holding potential. The kinetics of the current are not affected by the addition of Aa1 to the preparation; it means that the block is a simple 'plugging mechanism', in which a single toxin molecule finds a specific receptor site in the external vestibule of the  $K^+$  channel and thereby occludes the outer entry to the  $K^+$  conducting pore. © 2000 Elsevier Science B.V. All rights reserved.

**Keywords:** Amino acid sequence; *Androctonus australis*; Cerebellum granular cell;  $K^+$  channel; Patch-clamp; Scorpion toxin

### 1. Introduction

Review of recent literature shows an increasing interest in the search and use of venom components

as tools for neurobiological studies [1–5]. For example, the knowledge of the structure and function of potassium channels has been greatly increased by the discovery of specific natural peptide inhibitors used as probes at the molecular level [6–8]. The neurotoxic peptides, found in scorpion venoms, act specifically as high-affinity  $K^+$  channel blockers [3,9–11]. They have proven to be useful tools for channel purification [12–14], for structure–function analysis of voltage-gated and  $Ca^{2+}$ -activated  $K^+$  channels [15–18] and for the pharmacological classification of the different  $K^+$ -channel currents [1,19,20]. From the venom of North-African and Middle-East scorpions sev-

\* Corresponding author. Fax: +39-10-647-5575;  
E-mail: [presti@icb.ge.cnr.it](mailto:presti@icb.ge.cnr.it)

<sup>1</sup> These authors contributed equally to the paper.

<sup>2</sup> Also corresponding author. Fax: +52-73-172388;  
E-mail: [possani@ibt.unam.mx](mailto:possani@ibt.unam.mx)

eral such peptides have been isolated and characterized, from which Charybdotoxin has been the most widely studied [8]. *Androctonus mauritanicus* scorpion venom contains a toxin, P05, which is structurally and functionally similar to the leiurotoxin I (from the scorpion *Leiurus quinquestriatus*), a blocker of the apamin-sensitive  $\text{Ca}^{2+}$ -activated  $\text{K}^+$  channels [21]. Similarly, Kaliotoxin and Agitoxin are peptides from scorpions of the species *A. mauritanicus mauritanicus*<sup>3</sup> and *L. quinquestriatus* var. *hebraeus* [1,10], respectively, used to characterize several types of  $\text{K}^+$  channels.

In this communication, we report the amino acid sequence and the electrophysiological characterization of a peptide that we decided to call Aa1 (because it is peptide 1 of our studies, from the venom *A. australis* Garzoni). Structural features show that it belongs to group 4, and should be given the systematic number alpha KTX4.4, as discussed below. It entirely blocks only one type of  $\text{K}^+$  currents from cerebellum granular cells. The membrane of these cells contains several types of potassium channels with different kinetics and pharmacology [22]. Using the patch-clamp technique in the whole-cell configuration system, we have characterized the outward potassium currents. Two different currents were recorded: a fast transient, low-voltage activated current ( $I_A$ ), blocked by 4-aminopyridine (4-AP), which decays to a steady-state current level in about 100 ms due to the second component. It has electrophysiological and pharmacological properties similar to the classical squid axon potassium current ( $I_d$ ) [22]. Peptide Aa1 was shown to block specifically only the fast  $\text{K}^+$  currents of these cells.

## 2. Materials and methods

### 2.1. Materials

*A. australis* Garzoni (AaG) scorpion venom was purchased from Latoxan (Rosans, France). The culture medium was from Gibco (Rockville, MD, USA). Water double distilled on quartz was used for all experiments. Reagents and solvents used for chromatography and electrophysiological experiments were analytical grade, obtained as previously described [23].

### 2.2. Separation procedure

One hundred milligrams of venom from AaG was dissolved in 8 ml of double distilled water, centrifuged at  $15\,000\times g$  for 15 min and the supernatant was lyophilized and kept at  $-20^\circ\text{C}$  until used. The various active fractions used in this work were obtained by chromatographic separations, as previously described [23]. Briefly, the soluble venom was initially applied to a Sephadex G-50 column. The subfraction corresponding to the peptides of interest (range 4000 molecular mass) were further separated on carboxymethyl-cellulose (CM-cellulose) ion exchange resins, followed by high-performance liquid chromatography (HPLC). Peptide concentration was estimated on absorbance at 280 nm, in which one absorbance unit, using 1 cm pathlength was considered to contain 1 mg/ml peptide.

### 2.3. Amino acid sequence determination

Amino acid analysis was performed using a Beckman 6300E analyzer (Palo Alto, CA, USA) on samples hydrolyzed for 20 h, at  $110^\circ\text{C}$ , in sealed and evacuated tubes, in the presence of 6 N HCl and 0.2% phenol for protection of tyrosines. A mass spectrometer Voyager-DE STR from PerSeptive Biosystems (Framingham, MA, USA) was used for determination of the molecular mass and for analyzing the mass changes after hydrolysis using the Sequazyme C-Peptide Sequencing Kit from the same company (PerSeptive Biosystems). Amounts of about 0.5  $\mu\text{g}$  of toxin Aa1 were used for individual assays following the manufacturer's conditions. Additional hydrolysis of toxin was performed with the following enzymes: Protease V8 from *Staphylococcus aureus*, Arg C and Lys C endopeptidases (all from Boehringer Mannheim, Mannheim, Germany). The digestion with protease V8 was conducted in 100 mM ammonium bicarbonate buffer, pH 7.9, using 40  $\mu\text{g}$  toxin, whereas the digestion with Lys C endopeptidase was done in 25 mM Tris-HCl buffer, pH 8.5 added of 1 mM EDTA, with 30  $\mu\text{g}$  toxin. The hydrolysis with Arg C peptidase was performed with 5  $\mu\text{g}$  toxin in 100 mM Tris-HCl, pH 7.6 in the presence of 10 mM  $\text{CaCl}_2$ , 2.5 mM DTT and 0.25 mM EDTA. The ratio enzyme:toxin, was always 1:20. The incubation of the reaction was maintained for

4 h at 36°C. The products were separated by HPLC, using a Millennium 2010 system from Waters (Millford, MA, USA) equipped with a photodiode array detector, and the separation gradient was from solvent A (0.12% trifluoroacetic acid in water) to 60% B (0.1% trifluoroacetic acid in acetonitrile) for 1 h. All the peptides obtained were loaded into the Beckman-Porton LF3000 Protein Sequencer (Fullerton, CA, USA), for sequence determination. Repeated preparations were performed, in which aliquots of toxin were reduced and carboxymethylated, prior digestion with enzymes (v.g., protease V8 and Lys C endopeptidase). However, most sub-peptides were reduced and alkylated in the machine, using the protocol described by the manufacturer.

#### 2.4. Cell culture

Experiments were performed on cerebellum granular cells in primary culture obtained from 8-day-old Wistar rats. Dissociated cell cultures were prepared by trypsin digestion and mechanical trituration, following the procedure of Levi et al. [24]. Cells were plated at a density of  $2.5 \cdot 10^6$  per dish, on 35 mm plastic dishes or on glass coverslips, coated with 10 mg/ml poly-L-lysine and kept at 37°C in humidified 95% air/5% CO<sub>2</sub> atmosphere. Experiments were performed 5–10 days after plating.

#### 2.5. Patch-clamp measurements

Ionic currents were recorded in whole-cell patch-clamp technique configuration [25]. Patch pipettes were made from borosilicate glass (1.5 mm o.d., 1.17 mm i.d., from Clark Electromedical Instruments) and fire polished to obtain resistances between 2–4 MOhms. Cell responses were amplified and filtered at 2 kHz by an AxoPatch-1D (Axon Instruments). Both stimulation and data acquisition were performed with a 16-bit AD/DA converter (DigiData 1200, Axon Instruments) controlled by a computer PC 486. The whole-cell currents elicited by a 150–200 ms-long voltage steps between –60 and 80 mV from –50 and –80 mV holding potentials (HP) were acquired at a sampling time of 200  $\mu$ s. The capacitive transient component and series resistance of recorded currents were analog-compensated. When the voltage error associated with the uncom-

pensated series resistance was more than 10 mV, the membrane potential was corrected off line. P/4 leakage subtraction was performed on line. Data were stored on hard disk for subsequent analysis. The composition of the pipette filling solution was the following (in mM): 90 KF, 30 KCl, 2 MgCl<sub>2</sub>, 2 EGTA, 5 NaCl, 10 HEPES, 30 glucose, pH 7.35. The external standard solution, designed to suppress Na<sup>+</sup> and Ca<sup>2+</sup> currents, was (in mM): 135 NaCl, 2.5 KCl, 1 MgCl<sub>2</sub>, 1.8 CaCl<sub>2</sub>, 0.3 tetrodotoxin, 0.2 CdCl<sub>2</sub>, 10 HEPES, 10 glucose, pH 7.35. Purified peptides were directly added in the chamber containing 200  $\mu$ l of external solution.

All the experiments were carried out at room temperature ( $23 \pm 2^\circ\text{C}$ ).

### 3. Results

#### 3.1. Amino acid sequence determination

Results of the amino acid analysis showed that toxin Aa1 contains no histidine, leucine, phenylalanine or methionine and its minimum molecular weight was compatible with the presence of about 37–40 amino acid residues. Tryptophan cannot be determined in hydrolysates with HCl, but this amino acid was also shown to be absent by direct sequencing and molecular mass determination of the native peptide. Direct sequencing trials of the toxin gave no amino acid residues, confirmed that the N-terminal

1	10	20	30	37
-ZNETNKKCQG	GSCASVCRRV	IGVAAGKCIN	GRCVCYP	
-ETNKKCQG	GSCASVCRRV	IGVAAGKCIN	GR	
-		CIN	GRCV	
-			CVCY	
-		V	IGVAAGKCIN	GR
-				P
-ZN				

Fig. 1. Amino acid sequence of toxin Aa1. The overlapping amino acid sequences were obtained from HPLC separated peptides, as described in Section 2. Peptide from position 4 to 32 was obtained after protease V8 digestion, and glutamic acid at position 3, was surmised from the same enzymatic reaction (V8), whereas endopeptidase Arg C gave peptides from position 20 to 32 and 33 to 36. Lys C endopeptidase digestion produced peptide corresponding to positions 28–34. Position 37 was directly determined by mass spectrometry after digestion with carboxypeptidase Y, whereas positions 1 and 2 were obtained from a combination of amino acid analysis, mass spectrometry and sequencing results.

position was blocked [23]. Under digestion with protease V8, a sample of reduced and alkylated toxin gave a peptide, whose sequence identified 29 amino acids, shown below the full sequence in Fig. 1, which corresponds to amino acids in position 4–32 of the full sequence. Since the specificity of this enzyme supposes that the previous residue is a glutamic acid, in our experimental conditions, the amino acid in position 3, was surmised to be glutamic acid (see E in Fig. 1). One of the peptides obtained after digestion with Lys C endopeptidase gave the sequence starting at cysteine in position 28 to valine in position 34 (indicated in Fig. 1). Enzymatic cleavage with Arg C gave several sub-peptides one of them corresponded to the overlapping sequence from cysteine-33 to tyrosine-36, but gave also another peptide corresponding to sequence 20 to arginine-32. The last residue, proline-37, was obtained by mass spectrometry, after carboxypeptidase Y digestion. Three of the samples showed masses of 96.12, 97.09 and 97.04 which are consistent with the assumption that the last residue is proline. The first residue was assumed to be a pyroglutamic acid, based on the amino acid analysis, which showed a result compatible with the presence of more than two glutamic acids or glutamines in the sequence. It is worth remembering, that under acid hydrolysis, glutamine is eluted as glutamic acid. The value obtained in the amino acid analyzer, was compatible with the presence of more than two glutamic acids in the peptide (3.8 mol per toxin molecule). Thus, the presence of a pyroglutamic acid as first amino acid was assumed. The molecular mass obtained with native sample showed that the exact molecular mass of toxin Aa1 was 3850.83. When the 36 amino acids already positioned into the sequence were integrated, a value for the molecular mass of 3735.74 was found. The difference is 114.61 that fits with the mass of asparagine; for this reason, amino acid in position 2 was thought to be occupied by asparagine. This position for asparagine (or aspartic acid) is also partially supported by the results of amino acid analysis of the native toxin. The integrated value for aspartic acid plus asparagine, in toxin Aa1, was 2.45 per molecule (not shown), which means it could have two or three aspartic acids. It is convenient to remember that asparagine under acid hydrolysis gives aspartic acid. Since the molecular mass of the toxin obtained

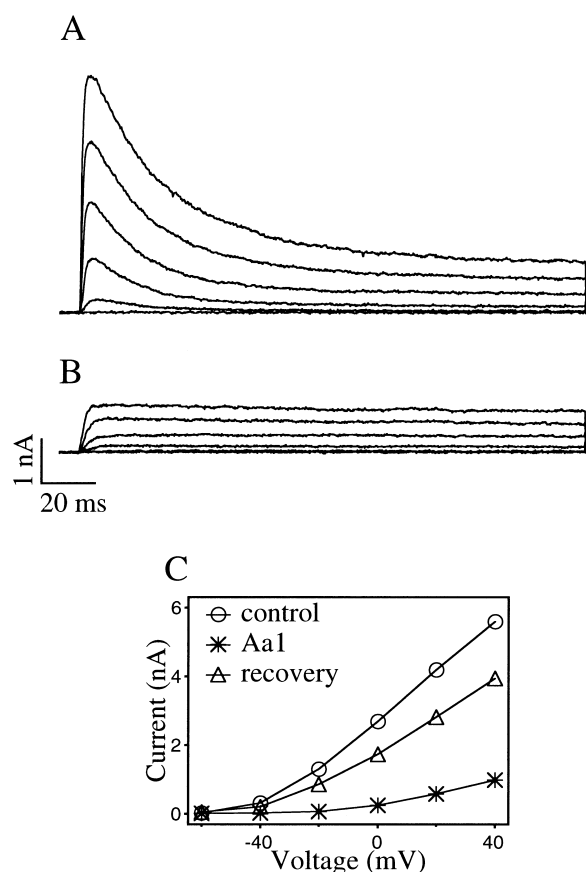


Fig. 2. Effect on  $I_A$  type  $K^+$  current Aa1 scorpion toxin acts on the  $I_A$  type potassium current selectively. (A) Family of control currents in response to voltage step from  $-60$  to  $+40$  mV in 20-mV increments. (B) Currents after bath application of  $2.7 \mu\text{M}$  Aa1. (C) Current-voltage relationship for peak  $I_A$  in control condition, in presence of  $2.7 \mu\text{M}$  Aa1 and after recovery.

by mass spectrometry suggested the lack of asparagine, we included this residue in position 2. Also, several other  $K^+$  channel scorpion toxins end by a tripeptide cysteine-tyrosine-proline, reason for placing asparagine in position 2, instead of 36, as discussed below.

### 3.2. Aa1 toxin blocks the transient $K^+$ channel in rat cerebellum granular cells

The purified peptide blocks currents flowing through the fast activating and inactivating  $K^+$  channels with high affinity only when applied to the extracellular side of the channel. Fig. 2 shows recordings from macroscopic  $K^+$  current elicited by depolarizing pulses in the control solutions (Fig. 2A), and after the addition of a saturating concentration ( $2.7$

$\mu\text{M}$ ) of Aa1 to the external solution (Fig. 2B). The  $I_A$  type component of the current was completely blocked while  $I_d$  type remains almost unaltered. The channels were activated by 200-ms pulses delivered at the rate of one every 5 s from an holding potential of  $-80$  mV, to allow a complete recovery from inactivation. Fig. 2C illustrates the current–voltage relationships for the peak. The recovery of the current after washing-out the toxin was never complete. At lower concentrations of Aa1 toxin and for perfusing periods of several minutes, the recovery did not overcome the 80% of control currents ( $60 \pm 20\%$ ,  $n = 25$ ).

### 3.3. Electrophysiological features of Aa1 toxin interaction with $I_A$ type current

We have studied the electrophysiological effects of this toxin on the kinetics of the fast activating and inactivating potassium current in order to elucidate the blocking mechanism. For this purpose, the  $I_d$  type potassium current was suppressed by 20 mM tetraethylammonium ion at the external side of the cell.

#### 3.3.1. Activation

The activation curve vs. membrane potential is shown in Fig. 3A. It represents the dependence of the open probability of channel from the test potential. It has been obtained calculating the ratio  $I/(V - V_{\text{rev}})$ , ( $V_{\text{rev}} = -97.5$  mV for potassium ion), and is fitted to a Boltzmann distribution  $I/I_{\text{max}} = 1/\{1 + \exp[(V - V_{0.5})/k]\}$ , where  $V$  is the test potential,  $V_{0.5}$  is the midpoint potential and  $1/k$  is the steepness of the curve. The best fit gave a  $V_{0.5}$  of  $1 \pm 3$  mV with a  $1/k$  value of  $0.051 \text{ mV}^{-1}$  in the control condition, whereas in the presence of Aa1 toxin, the  $V_{0.5}$  was  $2 \pm 2$  with a  $1/k$  value of  $0.043 \text{ mV}^{-1}$ . Thus there are no significative differences between the parameters in the control and toxin-containing conditions. Another important value to describe the activation kinetic of the current is the time between the starting potential pulse and the maximum of the current (time-to-peak, Fig. 3B). The toxin does not alter the rate of rise of the peak current.

#### 3.3.2. Inactivation

The steady-state inactivation process ( $h_{\infty}$ ) was

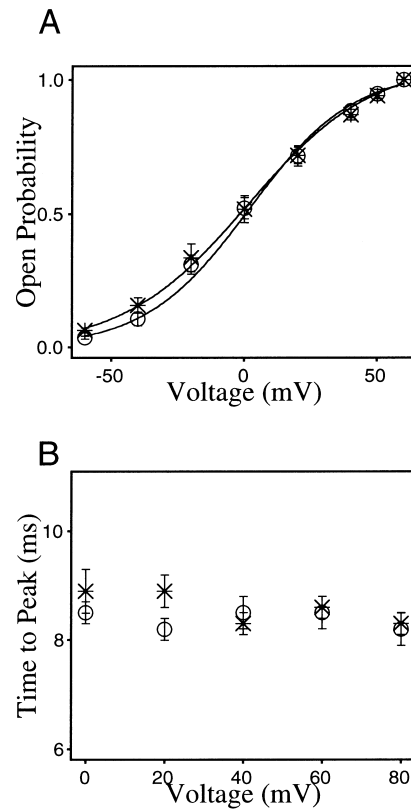


Fig. 3. Current activation kinetics Aa1 80 nM does not influence current activation kinetics. (A) Open probability of  $\text{K}^+$  channels vs. test potential. (B) Time-to-peak for transient current from HP =  $-90$  mV (mean  $\pm$  S.D.  $n = 7, 8$ ).

studied by using a two-pulse protocol (inset of Fig. 4A) consisting of a 480 ms-long prepulse from  $-120$  to  $-30$  mV, stepped by 10 mV, followed by a 50-ms-long test pulse to 50 mV.  $\text{K}^+$  channel availability was evaluated as the ratio  $I/I_{\text{max}}$ , namely the ratio between each current dependent on different preconditioning potentials and the maximum current corresponding to a  $-120$  mV preconditioning pulse. Fig. 4A gives the  $I/I_{\text{max}}$  values vs. voltage curve, fitted to a Boltzmann equation. Value for  $V_{0.5}$  was  $-73 \pm 0.6$  mV with a  $1/k$  of  $0.12 \text{ mV}^{-1}$  in the control condition, whereas in the presence of toxin, it was  $V_{0.5}$  of  $-78.8 \pm 0.8$  mV, with a  $1/k$  value of  $0.1 \text{ mV}^{-1}$ . Aa1 at the concentration 80 nM only marginally shifts the curves towards more negative potential (5.8 mV at the half-inactivated point). The recovery time from inactivation (Fig. 4B) was evaluated after a depolarizing prepulse to 0 mV for 0.5 s and a long-variable pulse to  $-90$  mV where the channels reactivate (inset of Fig. 4B). The value  $I/I_{\text{max}}$  was measured to +50

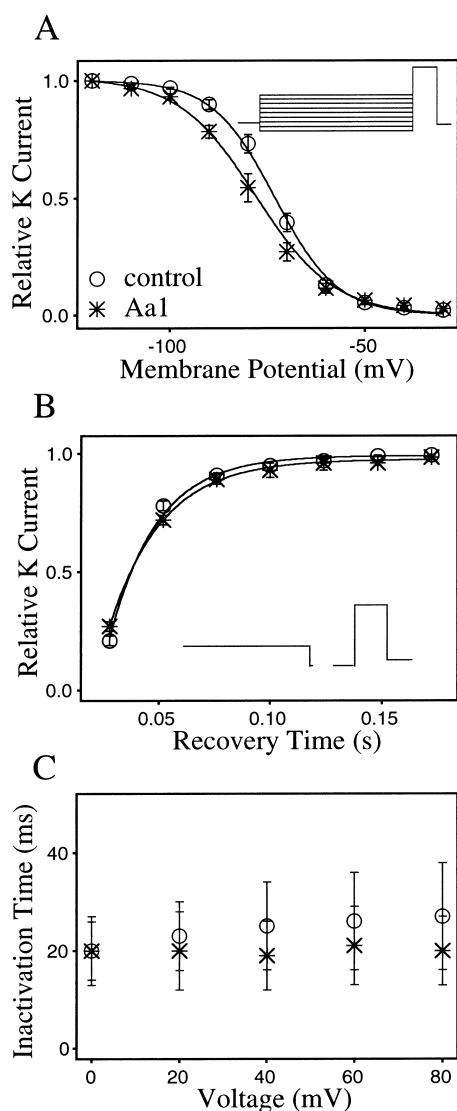


Fig. 4. Aa1 effects on current inactivation kinetics. (A) Steady-state inactivation curves for granular cells before and after exposure to 80 nM Aa1. Data represents peak  $I_A$  (mean  $\pm$  S.D.,  $n=7$ ) at +50 mV after a 0.48-s prepulse to the indicated potential. Experimental points were fitted to the Boltzmann equation (see text). (B) Normalized time course of  $I_A$  reactivation at -90 mV after a depolarizing prepulse to 0 mV for 0.5 s. (C) Inactivation time constant vs. depolarizing pulses.

mV test potential and plotted vs. the length of the -90 mV variable pulse in control situation and after adding Aa1 80 nM. Inactivation time courses of the transient current were found to be voltage independent and could be fitted by one exponential curve. The inactivation time constants in control experiments and in the presence of the toxin were plotted vs. voltage in Fig. 4C. The invariance of the last two

results confirm that the shift on the  $h_\infty$  is not significant.

### 3.3.3. Voltage dependence

Many toxins show different affinities for the binding site when different potentials are applied to the membrane. It is probably due to an electrostatic interaction between the electric charges present on the toxin surface and the voltage drop across the pore [9,26].

To study the voltage dependence, experiments were performed by varying the holding potential and observing the degree of blockade at a fixed test potential. The holding potential results show no significant differences on the extent of blockade and the depolarized test voltage does not influence Aa1 block (data not shown).

### 3.3.4. Closed channel block

The experiments of Fig. 5 were performed in order to assess the possible blocking effect of the toxin on closed channels [27]. The first test pulse applied after a very negative holding potential at -90 mV after 5 min from toxin addition, greatly reduced open channel probability. Exponentials were fit to the decay of each trace in Fig. 5 and extrapolated to the beginning of the voltage step to estimate the degree of block before channel opening. A 45% block precedes macroscopic activation during the 5 min. of exposure to 90 nM Aa1. The following voltage step, delivered 1 min later (6 min) elicited the same current: the blockade did not increase after the activation of the channel with the first pulse after 5 min of perfusion in the presence of the toxin. Thus the Aa1 peptide

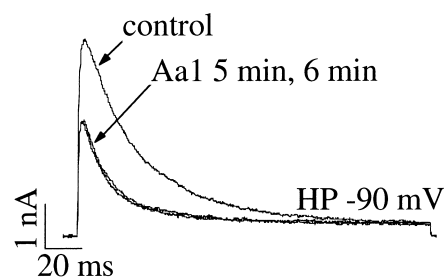


Fig. 5. Blockage of closed and open channels. Aa1 block of 'closed' channels is not influenced by channel opening: records represent consecutive and exclusive current response at +40 mV after control condition and after 5 min and 6 min of exposure to 90 nM Aa1. HP = -90 mV.

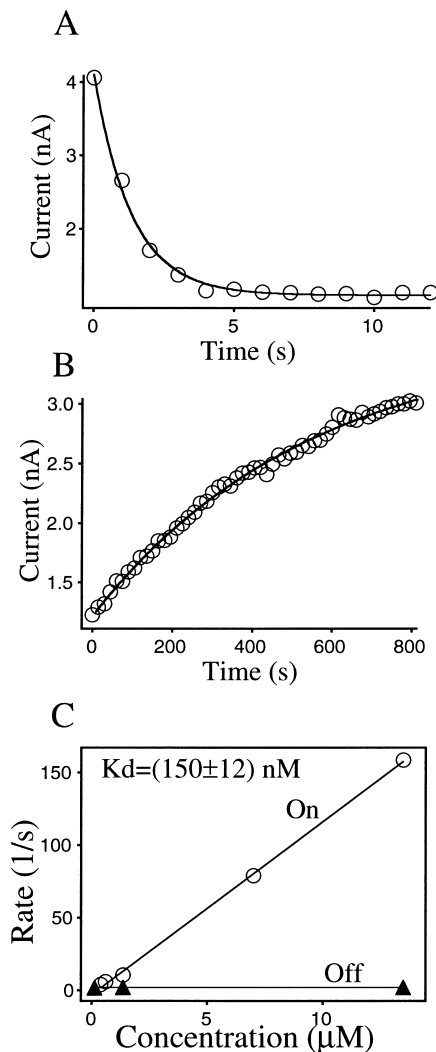


Fig. 6. Effect of Aa1 on blocking kinetics. (A) Peak current during toxin wash-in is plotted vs. time. (B) Time course of peak current during toxin wash-out. (C) The apparent first-order rate constant for association (on,  $K_{on}[Aa1]$ ) and dissociation (off,  $K_{off}$ ) are plotted as a function of toxin concentration. The slope of the line through the first-order association rate constant corresponds to a second-order association rate constant  $K_{on}$ .

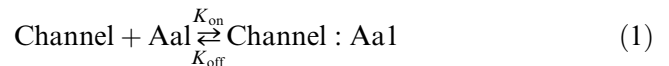
blocks the open and the closed channel independently.

### 3.3.5. The kinetics of toxin block

Fig. 6A and B shows the time courses of a multi-pulse wash-in/wash-out experiment using 270 nM of Aa1 toxin. The cell was held at  $-80$  mV and then repeatedly depolarized to  $40$  mV to assess unblocked current level. In this experiment, pulse of  $200$  ms

were collected at  $5$  s intervals. Plots of unblocked current vs. time are well fitted by single exponential functions for both toxin wash-in and wash-out.

Since toxin binds in reversible manner and does not alter channel gating, the time constants for relaxation to equilibrium block reflects the progress of the binding reaction. The Aa1 reaction with the binding site of the transient  $K^+$  channels, like the block of BK channels and the Shaker  $K^+$  channels by scorpion toxin, proceeds by the simple bimolecular reaction scheme:



where  $K_{on} = 11.9 \pm 0.3 \cdot 10^6 \text{ M}^{-1} \text{ s}^{-1}$  is the second-order association rate constant and  $K_{off} = 1.8 \pm 0.1 \text{ s}^{-1}$  the first-order dissociation rate constant. The time constant to approach to equilibrium blockade is given by  $\tau_{on} = 1/(K_{on}[Aa1] + K_{off})$  and that for wash-out is given by  $\tau_{off} = 1/K_{off}$ . The fraction of unblocked current at equilibrium ( $f_u$ ) in the presence of toxin concentration  $[Aa1]$ , is related to  $K_{on}$  and  $K_{off}$  according to  $f_u = K_{off}/(K_{on}[Aa1] + K_{off})$  and  $K_i = K_{off}/K_{on} = 150 \pm 12 \text{ nM}$ ; this last value is not significantly different from  $134 \pm 26 \text{ nM}$  shown in the paper by Pisciotto et al. [23]. Thus the desired rate and inhibition constants are estimated. Fig. 6C shows the effects of increasing toxin concentration on block kinetics. As required by simple bimolecular scheme, association rate increases linearly with toxin concentration, whereas the dissociation rate remains constant.

## 4. Discussion

The amino acid sequence reported here is consistent with the experimental data obtained. Direct sequencing confirmed amino acids in positions 3–36. The amino acids in positions 1, 2 and 37 are assumed based on amino acid analysis and molecular mass determinations. Asparagine (or aspartic acid as mentioned in Section 3) at position 2, could also be in position 36, shifting the positions one residue to the left on Fig. 1. In other words, position 2 would be glutamic acid and position 35 would be tyrosine, 36 asparagine and 37 proline. There is a remote possibility that the N-terminal pyroglutamic acid could be

1	10	20	30	40	
--ZNETNKK <b>C</b>	QGG <b>S</b> -CAS <b>V</b> C	RRV-IGVAAG	K <b>C</b> IN-GR <b>C</b> V <b>C</b>	YP-	Aa1 toxin
--ZF-TNV <b>S</b> C	TTSKE <b>C</b> WS <b>V</b> C	QRLHNTS-RG	K <b>C</b> MN <b>K</b> -K <b>C</b> R <b>C</b>	YS-	ChTx
--TI-INV <b>K</b> C	TSPK <b>Q</b> C <b>S</b> K <b>P</b> C	KELYGSSAGA	K <b>C</b> MN-GK <b>C</b> K <b>C</b>	YNN	NTx
--GVEINV <b>K</b> C	SGSP <b>Q</b> CL <b>K</b> P <b>C</b>	KDA--GMRFG	K <b>C</b> MNR-K <b>C</b> H <b>C</b>	TPK	KTx
---VFINA <b>K</b> C	RGSPE <b>C</b> LP <b>K</b> C	KEA-IGKAAG	K <b>C</b> MN-GK <b>C</b> K <b>C</b>	YP-	TsII-9 (TsKa)
-----AF <b>C</b>	NLRM-C <b>Q</b> L <b>S</b> C	RSL--G-LLG	K <b>C</b> IG-DK <b>C</b> E <b>C</b>	VKH	LeTxI (ScyTx)
-----LV <b>K</b> C	RGTS <b>D</b> CGR <b>P</b> C	QQQ-TGCPNS	K <b>C</b> IN-RM <b>C</b> K <b>C</b>	YGC	Pi1
-----TIS-- <b>C</b>	TNPK <b>Q</b> CY <b>P</b> H <b>C</b>	KKETGY <b>P</b> NA-	K <b>C</b> MN-RK <b>C</b> K <b>C</b>	FGR	Pi2 (PiTx Ka)
-----VS <b>C</b>	--ED-C <b>P</b> EH <b>C</b>	STQKA--QA-	K <b>C</b> DN-DK <b>C</b> V <b>C</b>	EPI	PO1
-----VG <b>C</b>	--EE-C <b>P</b> M <b>H</b> C	KGK-NAKPT-	-C <b>D</b> D-GV <b>C</b> N <b>C</b>	NV-	BmPO2
-----AV <b>C</b>	VYRT-C <b>D</b> K <b>D</b> C	KRR-GYRS-G	K <b>C</b> IN-NA <b>C</b> K <b>C</b>	YPY	CoTx1
--DEEPK <b>S</b> C	SDEM-C <b>V</b> I <b>Y</b> C	KGE-EY-STG	V <b>C</b> DGP <b>Q</b> K <b>C</b> K <b>C</b>	SD-	PbTx1
WCSTCLDL <b>A</b> C	GASRE <b>C</b> Y <b>D</b> P <b>C</b>	FKA-FGRAHG	K <b>C</b> MN-NK <b>C</b> R <b>C</b>	YTN	TsTx IV
----- <b>C</b>	----- <b>C</b>	----- <b>C</b>	----- <b>C</b>	----- <b>C</b>	---

Fig. 7. Amino acid sequence comparison of  $K^+$  channel-specific toxins. The primary structure of representative examples of each of the 12 subfamilies of alpha KTX scorpion toxins, taken from Tytgat et al. [28], are compared with toxin Aa1. Gaps (–) were artificially introduced in order to enhance identity. The percentage of identity found was: 40, 32, 37, 50, 29, 36, 22, 24, 19, 34, 21 and 27%, respectively, when calculated pairwise against toxin Aa1, for each one of the groups starting with group 1 until 12. The first sequence is from this work (Aa1 toxin), the others were from reference [31]: ChTx, charybdotoxin; NTx, noxiustoxin; KTX, Kaliotoxin; Ts II-9 or Kalpha, and TsTx IV, toxins from *T. serrulatus*; LeTxI, leiurustoxin-I or scyllatoxin; Pi1 and Pi2, toxin 1 and 2 from *Pandinus imperator*, BmPO2 toxin from *Buthus martensi*; toxin 2 from *Buthus indicus*; CoTx1, cobatoxin 1 from *C. noxius*; PbTx1, toxin 1 from *Parabuthus transvaalicus*.

some other modified amino acid that would sum up the molecular mass of asparagine. If we compare the amino acid sequence of Fig. 1 with data in the literature, it is evident that toxin Aa1 bears resemblance with other  $K^+$  channel specific toxins in its C-terminal amino acid sequence. Some of them have the terminal sequence cysteine–tyrosine–proline, just as toxin Aa1 of this work (see toxin Ts II-9 in Fig. 7, also toxin Clttx1 from *Centruroides limpidus limpidus* and the cobatoxins 1 and 2 from *Centruroides noxius*, reviewed in Possani et al. [2]).

In Fig. 7, we added a comparative table with the other known sequences, based on a recent publication, where a scientific nomenclature was proposed by a panel of international scientists working in this field [28]. According to this proposition, there are at least 12 different subfamilies of scorpion toxins specific for  $K^+$  channels, denominated alpha K scorpion toxins, from numbers 1 to 12, and sub-numbers according to the chronological discovery and report of the toxins. For Fig. 7, only one representative example of each subfamily was selected, and aligned with gaps (–) to increase similarities. Pairwise comparisons of toxin Aa1 with each one of the other 12 toxins gave an identity value relatively poor, which means that this toxin is quite different from all the other known ones, thus far in terms of total identity (see percentage in the legend for Fig. 7). The percentage of identity for toxin Aa1 found with other toxins

varies from 19 to 50%, when calculated for each one of the groups starting with number 1 until 12. The closest one is group 4, that gave 50% identity to toxin II-9 (also called Kalpha) from *Tityus serrulatus* [28]. A novel toxin belonging to this group was reported recently, which was classified as alpha KTx4.3, isolated from the venom of the scorpion *Tityus discrepans* [29]. Thus, the scientific number of toxin Aa1 should be alpha KTx4.4. It is worth observing that only six residues, all cysteines, are identical (see consensus sequence at the bottom of Fig. 7). It also should be mentioned that a novel class of scorpion toxins was discovered recently: Ergtoxin, specific for ERG  $K^+$  channels [30], with no similarities to any one of the toxins listed in the 12 subfamilies mentioned [28], for this reason, it was not included in our comparison of Fig. 7.

Concerning the physiological action, the results described here indicate that toxin Aa1, isolated from the scorpion venom *A. australis* Garzoni, affects the fast activating and inactivating  $K^+$  current in cerebellar granule cells. The toxin, added to the external solution, reduces in a selective manner the  $I_A$ -type component with a  $K_i = 150 \pm 12$  nM. In the same conditions, the other  $K^+$  current, identified as delayed rectifier ( $I_d$ ), was not affected. The recovery is not fully reversible. Long-lasting washing partially removes the block, very likely due to the run-down of the currents occurring in the mean time.



We have investigated the mechanism of block by Aa1 and the most relevant features are the following: (a) the kinetics of the channels are not affected by Aa1; (b) the blockade is independent of the test potential and is not affected by changing in holding potential; (c) the toxin inhibits the channel both in open or closed state; and (d) the blockade reflects the formation of a bimolecular toxin–channel complex, where the second-order association constant  $K_{\text{on}}$  is  $11.9 \pm 0.3 \cdot 10^6 \text{ M}^{-1} \text{ s}^{-1}$ , increasing linearly with toxin concentration and the dissociation rate  $K_{\text{off}}$   $1.8 \pm 0.1 \text{ s}^{-1}$  remains constant.

These results support the conclusion that toxin Aa1 blocks the transient  $\text{K}^+$  channels of the cerebellum granular cells in a simple bimolecular and pore-directed binding fashion. This mechanism of blockade resembles that described for other  $\text{K}^+$  channels by MacKinnon and Miller [11] and Giangiacomo et al. [19] using Charybdotoxin and Iberitoxin, respectively. Actually, toxin Aa1 has a blocked N-terminal amino acid (pyroglutamic acid), similar to Charybdotoxin and Iberitoxin, for which the primary structure identity is in the order of 40%. We are confident that Aa1 is a new example of a very interesting scorpion venom peptide, with exquisite preference for the transient  $\text{K}^+$  channels. The blockade of these channels, with no effect on  $I_{\text{d}}$  type of currents of the granular cells studied, shows its potential usefulness for specific  $\text{K}^+$  channels characterization. The  $K_{\text{i}}$  value for the transient  $\text{K}^+$  channels (150 nM), contrast with the effect on Shaker B potassium channel expressed in *Xenopus laevis* oocytes, where a  $K_{\text{i}}$  of 4.5  $\mu\text{M}$  was obtained for Aa1 [31].

Thus, we conclude that toxin Aa1 is a new and valuable ligand to recognize different subtypes of fast activating and inactivating  $\text{K}^+$  channels and will also provide an interesting instrument to investigate the structure–function relationship of these voltage-dependent  $\text{K}^+$  channels.

## Acknowledgements

The authors are indebted to Mr. G. Gaggero, D. Magliozzi and Dr. Fernando Zamudio for their technical assistance, and Dr. M. Ottolia for helpful comments on this manuscript. This work was partially supported by a grant from the European Com-

munities CII\* CT94-0045 and CNR/CONACYT for international cooperation to G.P. and L.D.P.; grants from the Howard Hughes Medical Institute (75197-527107) and DGAPA-UNAM (IN-217997) to L.D.P.

## References

- [1] M.L. Garcia, M. Garcia-Calvo, P. Hidalgo, A. Lee, R. MacKinnon, *Biochemistry* 33 (1994) 6834–6839.
- [2] L.D. Possani, B. Becerril, M. Delepierre, J. Tytgat, *Eur. J. Biochem.* 264 (1999) 287–300.
- [3] L.D. Possani, B. Selisko, G.B. Gurrola, *Perspect. Drug Discov. Des.* 15/16 (1999) 15–40.
- [4] R. Rappuoli, C. Montecucco in: *Guidebook to Protein Toxins and their Use in Cell Biology*, Oxford Press, 1997, pp. 143–163.
- [5] H.H. Valdivia, L.D. Possani, *Trends Cardiovasc. Med.* 8 (1998) 111–118.
- [6] E. Carbone, E. Wanke, G. Prestipino, L.D. Possani, A. Maelicke, *Nature* 296 (1982) 90–91.
- [7] C. Miller, E. Moczydlowski, R. La Torre, M. Phillips, *Nature* 31 (1985) 316–318.
- [8] C. Miller, *Neuron* 15 (1995) 5–10.
- [9] S.A. Goldstein, C. Miller, *Biophys. J.* 65 (1993) 1613–1619.
- [10] A. Gross, R. MacKinnon, *Neuron* 16 (1996) 399–406.
- [11] R. MacKinnon, C. Miller, *J. Gen. Physiol.* 91 (1988) 335–349.
- [12] F. Noceti, A.N. Ramirez, L.D. Possani, G. Prestipino, *Glia* 15 (1995) 33–42.
- [13] G. Prestipino, H.H. Valdivia, A. Lievano, A. Darszon, A.N. Ramirez, L.D. Possani, *FEBS Lett.* 250 (1989) 570–574.
- [14] H. Rehm, M. Lazdunski, *Proc. Natl. Acad. Sci. USA* 85 (1988) 4919–4923.
- [15] M. Crest, G. Jacquet, M. Goia, H. Zerrouk, A. Benslimane, H. Rochat, P. Mansuelle, M.F. Martin-Eauclaire, *J. Biol. Chem.* 267 (1992) 1640–1647.
- [16] S.A. Goldstein, D.J. Pheasant, C. Miller, *Neuron* 12 (1994) 1377–1383.
- [17] P. Hidalgo, R. MacKinnon, *Science* 268 (1995) 307–310.
- [18] H.G. Knaus, R.O.A. Koch, A. Eberhart, G.J. Kaczorowski, M.L. Garcia, R.S. Slaughter, *Biochemistry* 34 (1995) 13627–13634.
- [19] K.H. Giangiacomo, E.E. Sugg, M. Garcia-Calvo, R.J. Leonard, O.B. McManus, G.J. Kaczorowski, M.L. Garcia, *Biochemistry* 32 (1993) 2363–2370.
- [20] S.A. Goldstein, C. Miller, *Biophys. J.* 62 (1992) 5–7.
- [21] J.M. Sebatier, H. Zerrouk, H. Darbon, K. Mebrouk, H. Benslimane, H. Rochat, M.F. Martin-Eauclaire, J. Van Rietschoten, *Biochemistry* 32 (1993) 2763–2770.
- [22] M. Robello, C. Carignani, C. Marchetti, *Biosci. Rep.* 9 (1989) 451–457.
- [23] M. Pisciotta, F.I. Coronas, L.D. Possani, G. Prestipino, *Eur. Biophys. J.* 27 (1998) 69–73.

- [24] G. Levi, M. Aloisi, M. Ciotti, V. Gallo, *Brain Res.* 290 (1984) 77–86.
- [25] O.P. Hamill, A. Marty, B. Sakmann, E. Neher, F.T. Sigurth, *Pflugers Arch.* 391 (1981) 85–100.
- [26] M. Nobile, V. Magnelli, L. Lagostena, J. Mochca-Morales, L.D. Possani, G. Prestipino, *J. Membr. Biol.* 139 (1994) 49–55.
- [27] P.K. Wagoner, G.S. Oxford, *Biophys. J.* 58 (1990) 1481–1489.
- [28] J. Tytgat, G.K. Chandy, M.L. Garcia, G.A. Gutman, M.F. Martin-Eauclaire, J.J. Van der Walt, L.D. Possani, *Trends Pharmacol. Sci.* 20 (1999) 444–447.
- [29] G. D'Suze, F. Zamudio, F. Gomez-Lagunas, L.D. Possani, *FEBS Lett.* 456 (1999) 146–148.
- [30] G.B. Gurrola, B. Rosati, M. Rocchetti, G. Pimienta, A. Zaza, A. Arcangeli, M. Olivotto, L.D. Possani, E. Wanke, *FASEB J.* 13 (1999) 953–962.
- [31] M. Pisciotta, M. Ottolia, L.D. Possani, G. Prestipino, *Biochem. Biophys. Res. Commun.* 242 (1998) 287–291.